ISBN: 978-3-95450-132-8 doi:10.18429/JACoW-IPAC2014-TUPRI020

# STUDY OF ELECTRON CLOUD EFFECTS IN SUPERKEKB

Kazuhito Ohmi, Demin Zhou
KEK, 1-1 Oho, Tsukuba, 305-0801, Japan

*Abstract*

In SuperKEKB, high beta section exists in the interaction region. Fast head-tail instability and incoherent emittance growth due to electron cloud are enhanced in the high beta section. Especially high beta sections are located every betatron phase advance $\pi$. Nonlinear force due to electron cloud is coherently accumulated. Incoherent eminence growth dominates.

## INTRODUCTION

SuperKEKB is designed based on very low emittance and very low beta function at Interaction Point. The emittance is $\varepsilon_{x/y} = 3.2/0.0086$ nm and the beta function at IP is $\beta_x^* = 3$ cm and $\beta_y^* = 0.3$ mm. The beta function of Interaction Region, both side of IP, is very high ($\beta \sim 3{,}000$ m) due to recoil of the low IP beta. Generally effects of external force to beam is proportional to $\beta$. Dynamics of electron motion depends on the beam size of beam. Electron cloud build up was estimated by the simulation code 'PEI'. Under the ante-chamber geometry and secondary yield $\delta_{2,max} = 1.3$, the electron density was $2\times10^{11}$ m$^{-3}$ without special care. Growth time of electron cloud induced coupled bunch instability was 40 turns. The electron density has been measured in KEK using many test chambers with coating, groove, and so on. The density was reduced 1/10 as shown in later. The electron cloud effect is manageable in conventional analysis. We discuss electro cloud induced single bunch instability with focusing the large beta function at IR.

## SINGLE BUNCH INSTABILITY

### *Constant Beta Model*

As first step, the single bunch instability is evaluated under the condition that electron cloud distributes uniformly and the beta function is constant, $\beta_{xy} \approx 10$ m, along the whole ring [1]. Electrons oscillate in the electric potential formed by a positron bunch. The frequency is expressed by

$$\omega_e = \sqrt{\frac{\lambda_p r_e c^2}{\sigma_y(\sigma_x+\sigma_y)}} = 2\pi\times 136\ \mathrm{GHz}. \qquad (1)$$

$\lambda_p$, which is the local line density of the positron bunch, is $N_p/\sqrt{2\pi}\sigma_z = 6.0\times10^{12}$ m$^{-1}$. The beam sizes are $\sigma_x = 196$ $\mu$m, $\sigma_y = 10$ $\mu$m and $\sigma_z = 6$ mm. For low emittance ring, the frequency increases due to the small beam size. The electrons oscillate more than 10 period ($\omega_e\sigma_z/c = 17$) during the passage of a positron bunch. The oscillation induces a short range wake field with the frequency, $\omega_e$. As the result, a fast head tail instability is caused. Horizontal motion is slower than vertical one, thus vertical instability is more serious than horizontal one. The threshold of the vertical single bunch (fast head-tail) instability is given by

$$\rho_{e,th} = \frac{2\gamma\nu_s\omega_e\sigma_z/c}{\sqrt{3}KQr_e\beta_y L} = 2.2\times10^{11}\ \mathrm{m}^{-3}, \qquad (2)$$

where $K = \omega_e\sigma_z/c = 17$ and $Q = min(\omega_e\sigma_z/c, 10) = 10$ are used.

The single bunch instability has been studied by simulating the beam-electron cloud interactions using code 'PEHTS'. The simulation is performed by the same method as the strong-strong beam-beam simulation. A bunch is sliced into many pieces ($> \omega_e\sigma_z/c$). Interaction between a bunch slice and electron cloud is evaluated by potential solver based on the particle in cell method. The synchrotron radiation damping and excitation are not taken into account to be clear the instability threshold in this section.

Figure 1 shows evolution of the vertical beam size and a snapshot of beam-electron motion. The threshold density is $3.8\times10^{11}$ m$^{-3}$ as seen in top picture. The bottom picture depicts motion of bunch slices and electron centroid during the interaction for $\rho_e = 4.2\times10^{11}$ m$^{-3}$ at 4000-th turn. Coherent motion of bunch slices and electron cloud is seen. The slice beam size is comparable with the centroid motion. This means that coherent instability is dominant for the emittance growth.

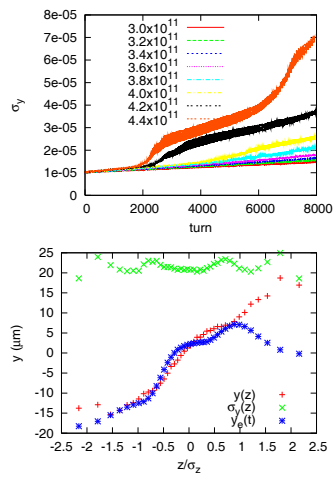


Figure 1: Evolution of the vertical beam size for various electron cloud density (top) and a snap shot of beam-electron motion (bottom).

These threshold values $2.1\times10^{11}$ (analytic) and $3.8\times10^{11}$ (simulation) are manageable for the electron build-up estimation [2].

ISBN: 978-3-95450-132-8 doi:10.18429/JACoW-IPAC2014-TUPRI020



### *Realistic Beta and Cloud Density*

The beam-electron cloud interaction depends on the local electron density and beam size. The frequency of electrons $\omega_e$ in Eq.(1) varies along $s$ respond to the beam size and/or beta function. $\beta_y$ characterizes coupling between beam-electron interaction as shown in Eq.(2). Tune shift caused by electron cloud is expressed by

$$\Delta\nu_y = \frac{r_e}{k\gamma}\rho_e\beta_y \tag{3}$$

where $k = 1$ or 2 for flat or round electron distributions, respectively.

SuperKEKB Vacuum group estimates electron density profile along $s$. Figure 2 shows the variation of $\beta_{x,y}$ and $\rho_e$. The density is around $0.2 \times 10^{11}$ m$^{-3}$ in most of the sections as shown in left picture. It is high at the symmetric point for IR. The density near IR is depicted in the right picture. Very high $\beta$ and dispersive sections are located near IR ($s$ = 27 and 68 m) for the local chromaticity correction. Bending magnets are located in the sections. Single bunch instability and nonlinear emittance growth are studied in two cases; (1) electron is not suppressed (green) and (2) is suppressed (cyan) at the high beta sections.

Figure 3 shows the vertical tune shift along the ring for the two cases. Tune shift, which arises in arc the section, is 0.0003, while that in IR is 0.0012 or 0.0009 for case (1) or (2), respectively. In either case, the tune shift in IR is dominant. Figure 4 shows electron oscillation phase $\omega_e\sigma_z/c$. The electron oscillation is 20 in arc, while is 5 or less in IR. The variation of $\omega_e$ reduces the quality factor of the wake force induced by electron cloud.

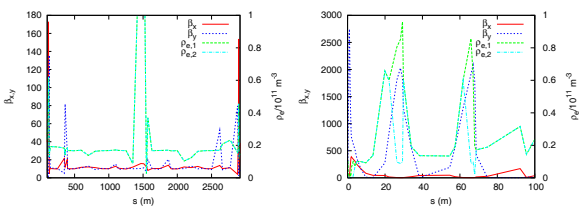


Figure 2: $\beta_y$ and electron central density $\rho_e$ along $s$. Left and right pictures depict whole ring and IR area, respectively.

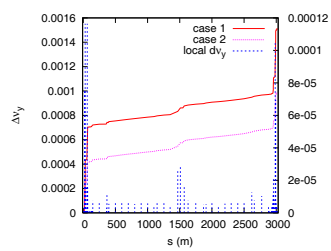


Figure 3: Vertical tune shift along the ring.

The beam-electron cloud simulation has been done under the beta and cloud density profile. Figure 5 shows the evolution of the vertical beam size for various electron cloud density. Top and bottom pictures depict beam size evolution for the cases (1) and (2), respectively. The threshold is 4× or 6× of the design for the cases (1) and (2), respectively.

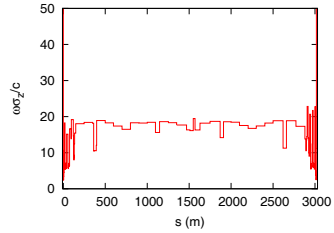


Figure 4: Variation of electron oscillation phase $\omega_e\sigma_z/c$.

We investigate which electron clouds in arc or IR is dominant for the instability. Figure 6 shows instability threshold caused by electron cloud in IR (top picture) or arc (bottom picture). The threshold density is $4-5\times$ or $20\times$ of the design for electrons only in IR or only in arc, respectively. Here electron cloud distribution of the case (1) is examined. The contribution of $\int \rho\beta_y ds \propto \Delta\nu_y$ is 4:1 as shown in Fig.3. The threshold densities are consistent with the ratio of $\int \rho\beta_y ds$.

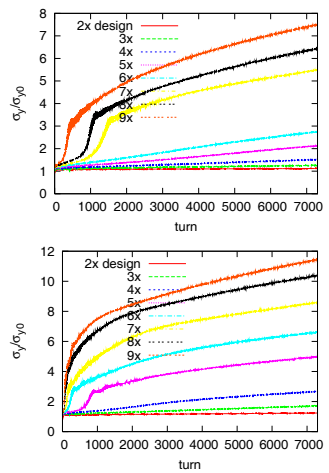


Figure 5: Evolution of the vertical beam size for various electron cloud density. The relative density distribution is given in Fig. 2.

## NONLINEAR EMITTANCE GROWTH

Emittance growth is seen bellow the threshold of the fast head-tail instability in Fig. 5. The emittance growth is caused by nonlinear force of the electron cloud charge distribution [3]. Electrons in IR were dominant for the tune shift and instability. Particles were tracked with a short time step $\Delta s \ll \beta_y$ in IR section. The short step is essential for prediction of the incoherent emittance growth correctly, because nonlinear effect was integrated by

$$\int K_n \beta_{xy}^{n/2} \exp(-in\phi_{xy}) ds, \tag{4}$$

ISBN: 978-3-95450-132-8 doi:10.18429/JACoW-IPAC2014-TUPRI020

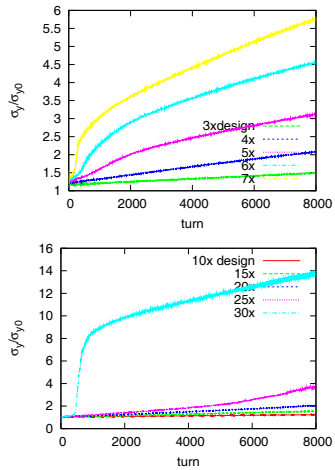


Figure 6: Evolution of the vertical beam size for various electron cloud density. In the top picture, electrons distribute only IR, $s < 75$ and $s > 2940$ m. In the bottom picture, electron distribute only in arc section, $75 < s < 2940$ m. The electron cloud distribution is the case (1).

where $F_n$ is strength of nonlinear force in Hamiltonian, $H = K_n x^n$.

Figure 7 shows the variation of $\beta_y$ and its phase in IR section. Locations with very high $\beta_y$ are separated with the phase $\pi$. Since electron transverse distribution is considered to be symmetric for $y$, the nonlinear effect is accumulated every high $\beta_y$ locations (note $n$ is even in Eq.(4).

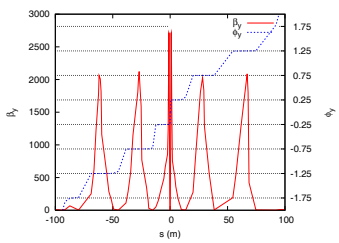


Figure 7: Vertical beta function and betatron phase variations in IR section.

To evaluate equilibrium emittance for the nonlinear growth, the radiation damping and excitation is taken into account in the simulation. The vertical radiation damping time is 4300 turns. Figure 8 shows the evolutions of the vertical beam size for various electron density. Top and bottom pictures depict the evolutions for the cases (1) and (2). The equilibrium beam size is realized after around several 1000 turns. The size is obtained as functions of the electron density. In the top picture, beam size evolutions above the threshold ($\rho_e = 5\times$ design) with (magenta) and without (black) synchrotron damping/excitation are plotted. It is found that the radiation damping somewhat suppresses the coherent single bunch instability.

Figure 9 shows the equilibrium emittance as function of electron density. The emittance increase is not serious for the design cloud density, but becomes serious for 3 times or higher than the design density.

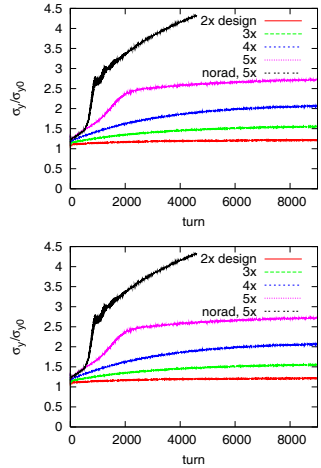


Figure 8: Evolution of the vertical beam size for various electron density. Top and bottom pictures depict the evolutions for the cases (1) and (2).

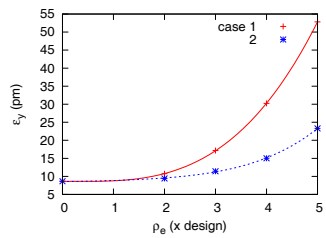


Figure 9: Equilibrium emittance as functions of the electron cloud density. Two lines, red and blue, are drawn for the cases (1) and (2), respectively.

## SUMMARY

Electron cloud instability based on the realistic electron distribution in SuperKEKB is summarized as follows,

- the vacuum system is designed so that electron density near the beam is suppressed around $2 \times 10^{10}$ m$^{-3}$ in average of whole ring,
- the threshold electron density is 4-6 times higher than the design,
- electrons near IR is dominant for the instability,
- emittance growth is negligible for $\rho_e \leq 2\times$ design.

## REFERENCES

[1] K. Ohmi and F. Zimmermann, Phys. Rev. Lett. 85, 3821 (2000).

[2] Y. Suetsugu et al., private comminications.

[3] E. Benedetto et al., Phys. Rev. Lett. 97, 034801 (2006).